NANO LETTERS

LETTER

pubs.acs.org/NanoLett

AC Field-Induced Polymer Electroluminescence with Single Wall Carbon Nanotubes

Jinwoo Sung,[†] Yeon Sik Choi,[†] Seok Ju Kang,[†] Sung Hwan Cho,[†] Tae-Woo Lee,[‡] and Cheolmin Park*[,†]

[†]Department of Materials Science and Engineering, Yonsei University, Seoul, Korea

[‡]Department of Materials Science and Engineering, Pohang University of Science and Technology (POSTECH), Pohang, Gyungbuk, Korea

Supporting Information

ABSTRACT: We developed a high-performance field-induced polymer electroluminescence (FPEL) device consisting of four stacked layers: a top metal electrode/thin solution-processed nanocomposite film of single wall carbon nanotubes (SWNTs) and a fluorescent polymer/insulator/transparent bottom electrode working under an alternating current (AC) electric field. A small amount of SWNTs that were highly dispersed in the fluorescent polymer matrix by a conjugate block copolymer dispersant significantly enhanced EL, and we were able to realize an SWNT-FPEL device with a light emission of approximately 350 cd/m^2 at an applied voltage of ±25 V and an AC frequency of 300 kHz. The brightness of the SWNT-FPEL device is much greater than those of other AC-based organic or even inorganic ELs that generally require at least a few hundred volts. Light is emitted from our SWNT-FPEL device because of the sequential injection of field-induced holes and then electron carriers through ambipolar carbon nanotubes under an AC field, followed by exciton formation in the conjugated organic layer. Field-induced bipolar charge injection provides great material design freedom for our devices; the energy level does not have to be aligned between the electrode and the emission layer, and the balance of the carrier injected and transported can be altered in contrast to that in conventional organic light-emitting diodes, leading to an extremely cost-effective and unified device architecture that is applicable to all red−green−blue fluorescent polymers.

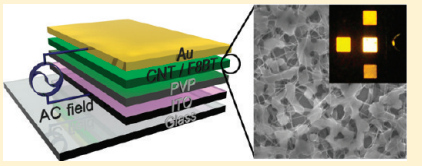

KEYWORDS: Field-induced electroluminescence, fluorescent polymers, single wall carbon nanotubes, alternating current, nanocomposites

Organic conjugated molecules are of great interest in electroluminescence (EL) research because of their high quantum efficiencies arising from the radiative decay of excitons.[1,2] In particular, light-emitting polymers have attracted great attention because they can be easily integrated into EL devices using solution processes under ambient conditions.[3,4] Because EL of organic conjugated molecules is in principle achieved through the recombination of holes and electrons injected from their own ohmic electrodes in the emissive layer,[1,3,4] a device with high EL efficiency should guarantee plentiful injection of both electrons and holes, as well as their balanced recombination. These rather strict requirements have resulted in the use of elaborate material designs and complicated device structures containing cathodes, anodes, charge injection layers, charge blocking layers, and charge transport layers in organic light emitting diodes (OLEDs).[1,3−6] In organic light-emitting transistors (OLETs), a hole and electron-transporting bilayer and a hole-transporting/emitting/electron-transporting trilayer are additionally present.[7−9] Furthermore, the layers should have the appropriate electronic band structures to produce the colors desired in the emissive active layers.

New organic electroluminescence (OEL) devices with a simpler and more universal architecture are therefore in demand. Great efforts have been made to develop organic light-emitting devices with novel device structures and emission principles; devices based on alternating current (AC) electric fields are an example of such novel device structures. Thin conjugated organic films placed on an insulator or inserted between insulators emit light under the excitation of AC voltage, similar to inorganic electroluminescence (IEL).[10,11] The mechanism of OEL devices is based either on solid-state cathode luminescence (SSCL)[12−14] in which EL can be achieved through the impact excitation of organic phosphor after bombardment with hot electrons accelerated through an inorganic oxide layer or on field-induced luminescence in which bipolar charges injected from electrodes under an AC field form excitons and are then recombined in the conjugated organic layer.[15,16] Additional conductive layers such as thin metal films or indium tin oxide (ITO) nanoparticles in OEL devices have been shown to enhance EL because of the more effective generation of holes and electrons by these layers.[15,16]

OELs operating under an AC electric field are potentially stable because the insulating layer can prevent possible electrochemical reactions between the organic-emitting layer and the electrode. These devices are, however, far from being implemented in practice because of the very low charge carrier mobility of organic emitters as well as the high contact energy barrier between the electrode and organic materials. Consequently, the EL performances of these devices are quite low at very high

Received: September 30, 2010
Revised: January 15, 2011
Published: January 31, 2011

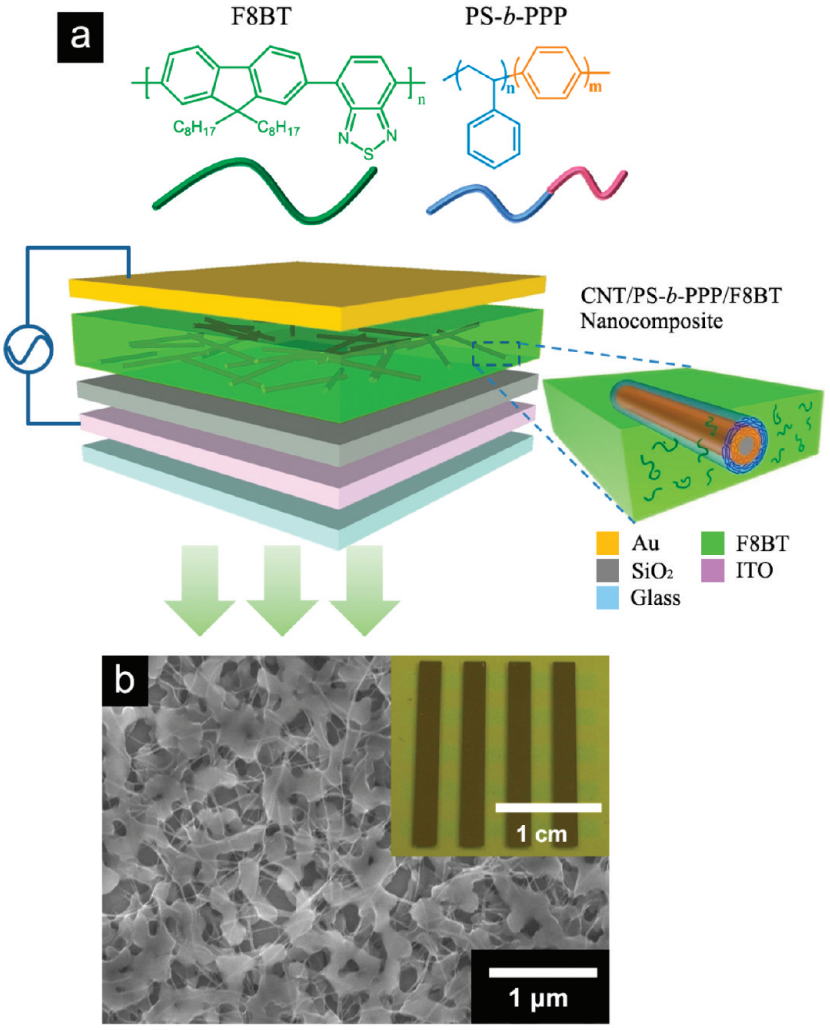

Figure 1. (a) Schematics of the device architectures of the SWNT-FPEL devices comprised of four layers: a SWNT/PS-*b*-PPP/light-emitting polymer nanocomposite layer, an insulator layer, and a transparent bottom electrode stacked on top of the metal electrode. The molecular structures of PS-*b*-PPP as a dispersant for SWNTs and of F8BT as a light-emitting polymer are shown. (b) An SEM image showing the morphology of a SWNT/PS-*b*-PPP/F8BT nanocomposite thin film spin-coated from THF solution containing 0.2 mg/mL SWNTs, 1 mg/mL PS-*b*-PPP, and 10 mg/mL F8BT. The inset of (b) shows a photographic image of a 4 × 4 array of SWNT-FPEL devices.

operation voltages (over 100 V).[12−16] Use of single wall carbon nanotubes (SWNTs) has led to breakthroughs in advanced photonic and electronic devices ranging from transistors to photosensors,[17] and unipolar or ambipolar SWNTs have been successfully incorporated into EL devices in the near-infrared (NIR) region to achieve a tunable emission wavelength.[18,19] On the basis of recent studies that demonstrated that the addition of SWNTs into emissive or transport layers in conventional OLEDs improved charge injection, leading to improved EL with a reduced threshold voltage,[20−23] we hypothesized that ambipolar SWNTs individually networked in a polymeric emitter would greatly enhance the performances of AC-driven OEL devices.

Here, we report a novel, high-performance OEL containing a thin nanocomposite film made of SWNTs dispersed in a light emitting-polymer matrix under an AC electric field. Our OEL device is based on facilitated field-induced luminescence in which holes and electrons are sequentially injected by the AC electric field from an electrode to networked SWNTs in the composite and are then subsequently transferred to light-emitting polymers, leading to greatly improved light emission. An AC field-induced polymer EL (hereafter denoted as SWNT-FPEL) device with SWNTs individually dispersed within the polymer matrix through solution processes emitted light with a brightness of approximately 350 cd/m^2 at a voltage of ±25 V and a frequency of 300 kHz. This level of brightness is much greater than those of other AC field-induced OELs and even recent state-of-the-art IELs, which typically operate at a few hundred volts.[24] Furthermore, the field-induced luminescence of our devices avoids various materials design issues that are associated with conventional OLEDs, such as the requirement for energy level alignment between the electrode and the emission layer and balancing of carrier injection and transport, resulting in an extremely cost-effective and unified device architecture that can be used to achieve full color.

Our SWNT-FPEL device consists of a top metal electrode and a thin nanocomposite film of SWNTs embedded in a light-emitting polymer matrix layered on top of the transparent bottom electrode with an insulating layer, as shown in Figure 1a. This device structure is similar to that of a metal/insulator/semiconductor/metal (MISM). To systematically investigate the

dx.doi.org/10.1021/nl103458g |*Nano Lett.* 2011, 11, 966–972

effect of SWNTs on SWNT-FPEL, we employed poly[(9,9-di-*n*-octylfluorenyl-2,7-diyl)-alt-(benzo[2,1,3]thiadiazol-4,8-diyl)] (F8BT) as an emissive layer in nanocomposite films with different amounts of SWNTs. The composite films were spin-coated from solutions of 10 mg/mL F8BT in tetrahydrofuran (THF) on a 200 nm thick SiO_2 insulator sputtered onto a patterned, transparent ITO bottom electrode. Concentrations of SWNTs ranging from 0.05 to 0.4 mg/mL that had previously been dispersed with 1 mg/mL poly(styrene-*b*-paraphenylene) (PS-*b*-PPP) were examined. PS-*b*-PPP is a conjugated block copolymer capable of efficiently dispersing SWNTs using dangling solvating blocks (PS) in solvent and anchoring conjugated blocks (PPP) to tube walls, as explicitly described in our previous study.[25] SWNTs individually dispersed and encapsulated by PS-*b*-PPP were well mixed with F8BT, leading to homogeneous composite films with thicknesses of approximately 200−250 nm. A typical microstructure of a SWNT/PS-*b*-PPP/F8BT nanocomposite film is shown in Figure 1b. Individually dispersed carbon nanotubes were apparent, while large aggregates of nanotubes were present in the composite film containing SWNTs and F8BT without PS-*b*-PPP, even after a long period of ultrasonication (see Supporting Information, Figure S1). Fabrication of a SWNT-FPEL device was completed when 2 mm wide periodic Au top electrodes were thermally deposited onto the nanocomposite film. A photograph of a 4 × 4 array of the device is shown in the inset of Figure 1b.

The UV−visible absorbance and photoluminescence (PL) behavior of the nanocomposites of SWNTs/PS-*b*-PPP/F8BT were investigated as a function of SWNT concentration, as shown in Figure 2. Addition of SWNTs to the films slightly increased the intensity of the characteristic F8BT absorbance peaks at 300 and 450 nm simply because of the increase in film thickness due to the SWNT-induced increase in the solution viscosity, as shown in Figure 2a,c.[26] In contrast, the PL intensity of the composite films at approximately 550 nm (Figure 2b) decreased with the addition of SWNTs when the films were excited with a 450 nm light source, which implies that excitons of F8BT were quenched because of exciton dissociation by electron-accepting SWNTs, Förster resonance energy transfer (FRET) from F8BT to SWNT, and/or nonradiative thermal dissipation.[27] Because this quenching could adversely impact EL in conventional OLEDs, the amount of SWNTs and their distribution in the films should be carefully optimized to ensure that PL properties are not too adversely affected, while at the same time maximizing field-induced bipolar charge generation to realize high performance SWNT-FPELs. For instance, an approximately 20% loss in PL in a nanocomposite film with 2 wt % SWNTs with respect to polymer concentration in Figure 2c was acceptable to realize the highest brightness, as we will describe below. Note that the UV−visible absorbance and the PL of nanocomposite films were almost completely dominated by F8BT due to the very minor contributions of both PS-*b*-PPP and SWNTs (see Supporting Information, Figure S2).

The EL performance of SWNT-FPELs was investigated as a function of both the amount of SWNTs present in the composites and the frequency of the square-pulsed ±40 V AC bias, as shown in Figure 3a. The characteristic light of F8BT with a wavelength of 550 nm, consistent with that of PL, was emitted at an increased frequency, and the intensity of this light was maximal at a frequency around 300 kHz in most of the nanocomposite devices regardless of the amount of SWNTs. Emitted light was detectable by eye in most of the SWNT-FPEL devices; a typical

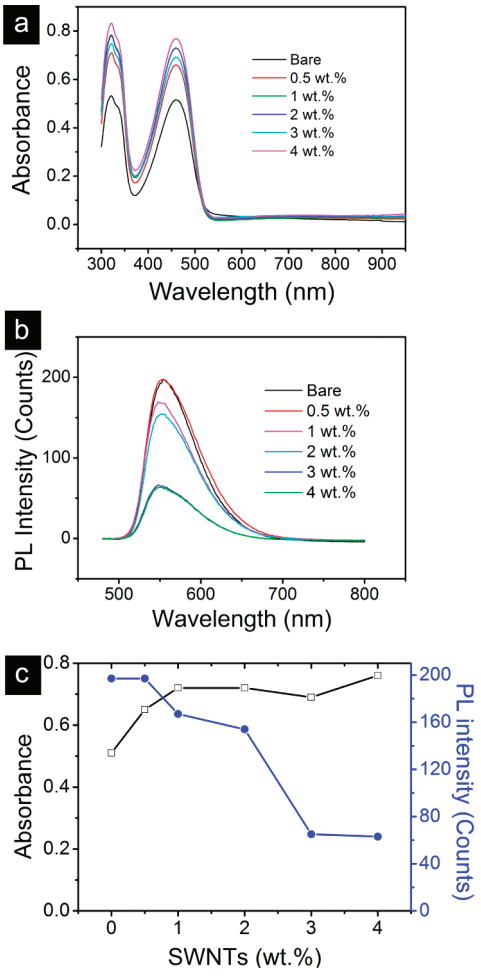

Figure 2. Optical properties of SWNTs/PS-*b*-PPP/F8BT nanocomposites spin-coated from THF solutions containing 1 mg/mL PS-*b*-PPP, 10 mg/mL F8BT, and SWNTs at concentrations ranging from 0.05 to 0.4 mg/mL. (a) UV−visible absorbance. (b) Photoluminescence obtained at an excitation wavelength of 450 nm. (c) Plots of UV−visible absorbance (left) and photoluminescence (right) as a function of SWNT concentration.

photograph is shown in Figure 3b. It should be noted that several cells in the proximity of the brightest one were simultaneously turned on due to cross-talk between cells, which we attribute to spreading of the electric field from the assigned electrode. The cross-talk between cells could potentially be suppressed by designing a new electrode architecture in which particular ITO cathodes are effectively separated. Cell-to-cell isolation could also be achieved through the micropatterning of F8BT/PS-*b*-PPP/SWNT nanocomposite films using various nondestructive printing techniques such as inkjet, transfer, or microimprinting techniques. The addition of SWNTs up to a certain concentration greatly enhanced the brightness of our devices, but EL performance tended to deteriorate when excess nanotubes were added to the composite films, as demonstrated in Figure 3a. The maximum brightness was approximately 200 cd/m^2 in the SWNT-FPEL device operating at 300 kHz with a nanocomposite film containing 2 wt % SWNTs with respect to F8BT. This value is much greater than that of pure F8BT film under the same conditions, as indicated in Figure 3a. The light emitted by the SWNT-FPEL devices increased almost linearly in intensity

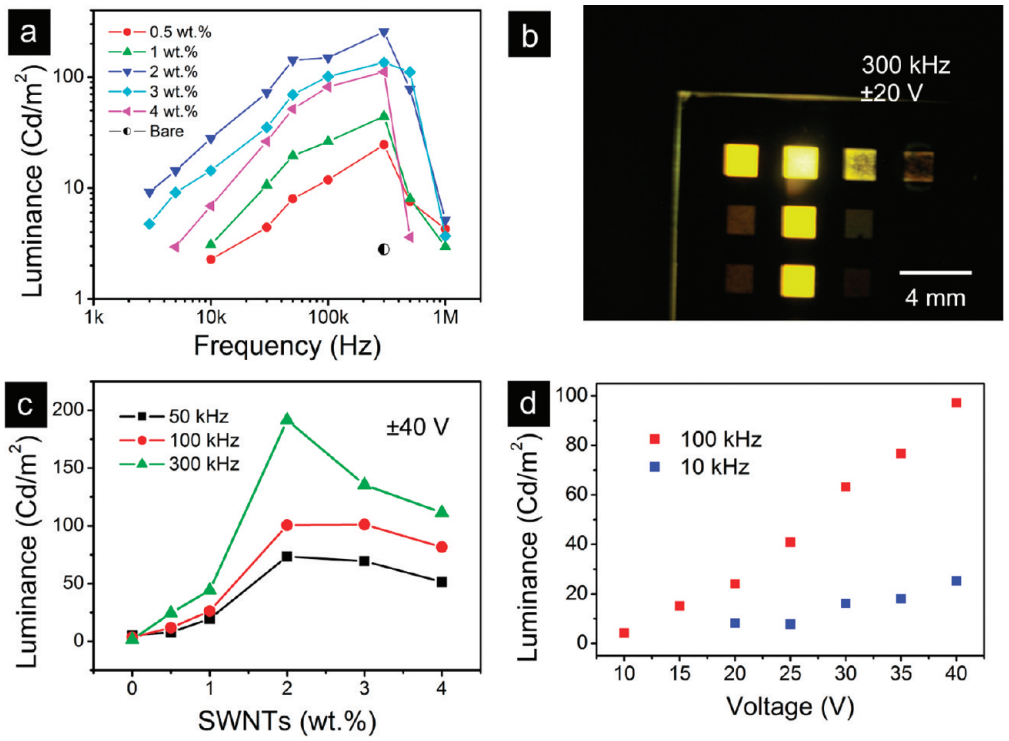

Figure 3. EL performances of the SWNT-FPEL devices consisting of Au/(SWNTs/PS-*b*-PPP/F8BT) nanocomposites/200-nm-thick SiO_2/ITO. (a) The brightness and frequency relationships of SWNT-FPEL devices with SWNTs ranging in concentration from 0.5 to 4 wt % with respect to F8BT. The driving AC voltage was ±40 V. The EL brightness of pure F8BT without nanotubes is also shown. (b) A photograph of a 3 × 4 array of SWNT-FPEL devices with 2 wt % SWNTs emitting the characteristic light of F8BT at 300 kHz. Several cells in the vicinity of the brightest one are simultaneously activated due to the lack of isolation between cells. (c) The brightnesses of the SWNT-FPEL devices as a function of SWNT concentration at the denoted frequencies and a driving voltage of ±40 V. (d) Plots of brightness and applied voltage for SWNT-FPEL devices with 2 wt % SWNTs at 10 and 100 kHz.

according to square-pulsed applied voltages up to approximately ±50 V, above which the voltage devices were electrically deteriorated, as shown in Figure 3d.

Light emission from a device containing pure F8BT, despite the very low intensity of this light, is produced through a field-induced bipolar luminescence mechanism. After one type of carrier (hole or electron) accumulates in F8BT after AC is applied, the polarity reversal of the AC field leads to injection of the other type of carrier (electron or hole), and both types of carriers meet to form excitons, leading to light emission upon recombination. The light intensity of the device with pure F8BT was very low, possibly because of the low intrinsic carrier density and the low mobility of F8BT and/or the high injection barrier from the top electrode to F8BT. We interpret the significant improvement in brightness achieved through the incorporation of SWNTs to be facilitated via field-induced EL, as illustrated by the scheme shown in Figure 4. SWNTs are ambipolar and capable of generating both holes and electrons under an AC electric field.[28] In addition, they have a much higher carrier mobility and a lower energy barrier with the electrode than do common organic semiconductors, including F8BT.[29] Either hole or electron carriers are therefore preferentially generated in SWNTs by the corresponding AC field, and these are subsequently transferred to the nearby F8BT layer that contains individually dispersed nanotubes, resulting in a large interfacial area of the conjugate polymer matrix. Furthermore, the high length to diameter aspect ratio of SWNTs greatly supports charge tunneling into F8BT through PS-*b*-PPP shielding nanotubes. When the polarity of the electric field is reversed, the opposite charge carriers are injected into SWNTs from the electrode and are subsequently transferred to F8BT, as shown in the middle schematic of Figure 4. The carriers form excitons with the other type of charge carrier injected previously, resulting in luminescence due to exciton recombination, as shown in the bottom illustration of Figure 4. Emission intensity therefore increases with AC frequency as well as with the number of nanotubes present in the composite films because of the increase in the number of charge carriers with both frequency and SWNTs up to certain levels, as observed in Figure 3. F8BT cannot respond to a frequency higher than 1 MHz because of its low intrinsic carrier mobility.

The deterioration in EL at high concentrations of nanotubes can be explained by various factors. Luminescence quenching by FRET of excitons from F8BT to SWNTs may occur when recombination sites are close enough to interact with nanotubes when the latter are present at a high concentration. More importantly, the deterioration of EL may be related to the dispersion of the nanotubes. The aggregation of nanotubes after a critical dispersion concentration is surpassed can cause significant fluorescence quenching of F8BT *via* exciton dissociation by electron-accepting SWNTs, similar to the PL results shown in Figure 2b. Independent conductivity measurements of the nanocomposite films as a function of SWNT number showed that conductivity was the highest at a SWNT concentration of 0.2 mg/mL and began to decrease above this concentration due to the formation of aggregates; a SWNT concentration of 0.2 mg/mL was the optimum dispersion concentration for our nanocomposites

dx.doi.org/10.1021/nl103458g |*Nano Lett.* 2011, 11, 966–972

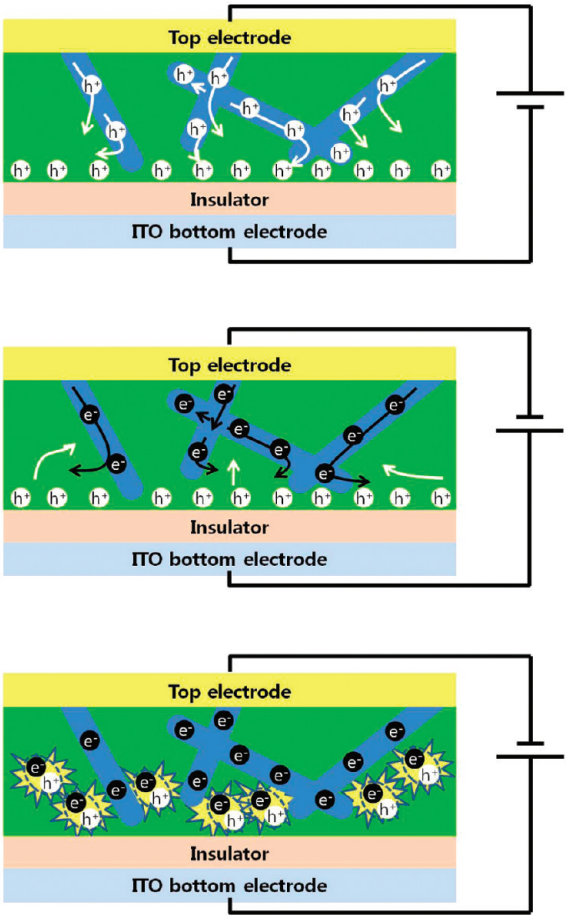

Figure 4. Schematics of the proposed mechanism of light-emission in SWNT-FPEL devices. When a positive field is applied to the top electrode, holes are injected into the carbon nanotubes because of their ohmic natures; these holes are in turn transferred to F8BT and preferentially accumulate at the F8BT/insulator interface (top scheme). The reversal of polarity results in the injection of electrons into the SWNTs, and these electrons drift toward the interface. Simultaneously, the previously accumulated holes move toward the carbon nanotubes (middle scheme). The holes and electrons in F8BT form excitons that subsequently emit light upon recombination (bottom scheme).

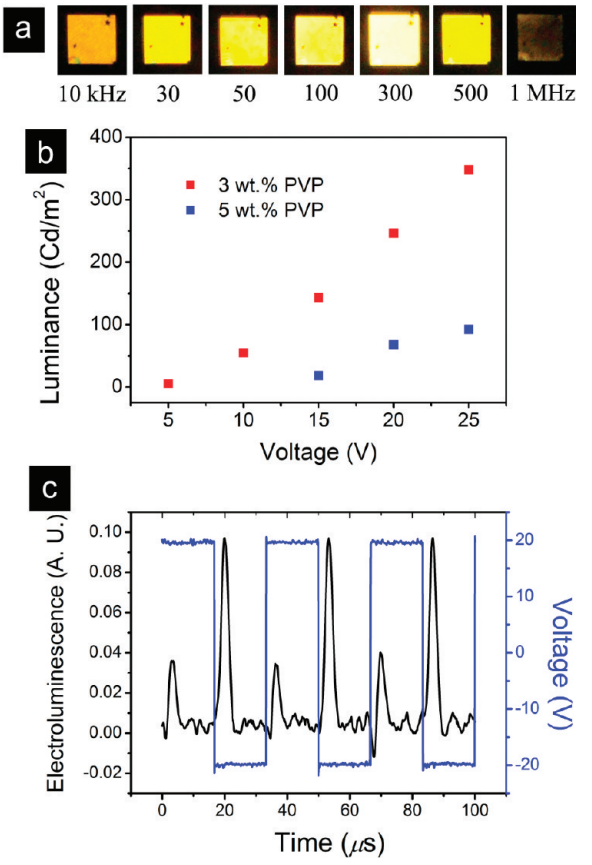

Figure 5. SWNT-FPEL devices with SWNTs/PS-*b*-PPP/F8BT nanocomposites prepared on PVP dielectrics. (a) Series of photographs of light emission from a SWNT-FPEL device with a nanocomposite containing 2 wt % SWNTs on a 200 nm thick PVP layer as a function of frequency at a driving voltage of ±25 V. (b) The brightness and voltage relationships of SWNT-FPEL devices on PVP dielectrics spin-coated using 3 and 5 wt % PVP solutions at a frequency of 300 kHz. (c) The time-resolved EL signal of the SWNT-FPEL device under successive ±20 V square-pulsed voltage trains.

(see Supporting Information, Figure S3). The EL performances of the devices as a function of SWNT concentration were qualitatively consistent with the dispersion of the nanotubes (Figure 3b). Our results imply that the deterioration of EL in SWNT-FPEL devices is greatly affected by the dispersion of nanotubes, and that it is crucial to have individually dispersed SWNTs within F8BT for high EL performance.

Contrary to SSCL or IEL, in which hot electrons in inorganic insulating layers are accelerated under an AC field,[12−14,30] the insulating layers in our SWNT-FPEL device functioned as dielectrics and increased the electric field for successive bipolar charge injection, transfer, and accumulation. This allowed us to employ a polymeric insulator that is barely capable of electron acceleration because of its extremely low charge mobility.[16] SWNT-FPEL devices with an approximately 200 nm thick poly(4-vinylphenol) (PVP) dielectric layer clearly exhibited frequency-dependent light emission similar to that observed with a SiO_2 layer. The series of photographs of SWNT-FPEL devices presented in Figure 5a show AC frequency-dependent light emission with square-pulsed voltage trains at ±25 V. When a PVP layer of approximately 100 nm in thickness was employed, light emission improved further, as shown in Figure 5b. Notably, the SWNT-FPEL devices yielded a light intensity of approximately 350 cd/m^2 at a frequency of 300 kHz and a voltage of ±25 V. These results strongly support our argument that the mechanism of light emission is field-induced luminescence. Note that the light emission of the SWNT-FPEL device with a thinner PVP layer (100 versus 200 nm thick SiO_2) was further enhanced because the higher capacitance PVP layer was capable of accumulating more charges than was the SiO_2 layer. Furthermore, the turn-on AC voltage of the device was significantly reduced to approximately ±5 V compared to the ±10 V required for the 200 nm thick SiO_2 layer (see Figure 3d). The luminescence of our device tended to decay continuously with operation time but remained stable after a certain time, similar to the behaviors of conventional polymer LEDs.[31] In general, the decay rate slowed at low frequencies and voltages. It should be noted that all device fabrication processes and measurements were performed under ambient conditions; no specific clean facility was used. We therefore believe that the emission stability of our device would improve significantly if the device were encapsulated in a polymer

dx.doi.org/10.1021/nl103458g |*Nano Lett.* 2011, 11, 966–972

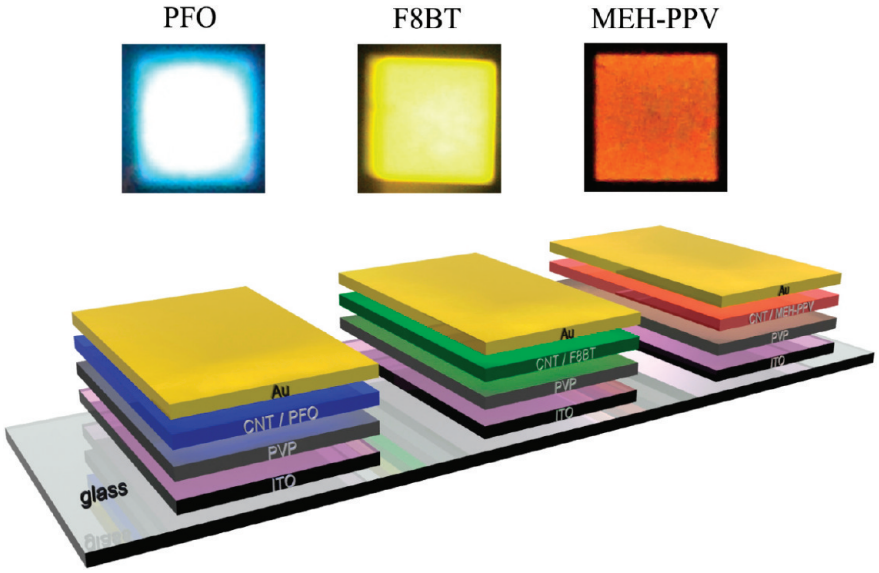

Figure 6. Photographs of SWNT-FPEL devices containing Au/(SWNTs/PS-*b*-PPP/fluorescent polymer) nanocomposite with a 2 wt % SWNT/100-nm-thick PVP/ITO architecture. PFO, F8BT, and MEH-PPV successfully produced ELs of blue, yellow, and red, respectively. To more clearly demonstrate red emission from the MEH-PPV device, we intentionally turned on the cell at a low frequency of approximately 10 kHz. The schematic shows the device platform in which the set of top and bottom electrodes and the insulating layer are universally applicable for all RGB colors.

resin, which would prevent direct contact with oxygen and water moieties. We are currently investigating the stability of this type of encapsulated device.

The temporal behavior of the light emitted from the SWNT-FPEL device upon AC excitation further confirmed the field-induced operation of our devices. A SWNT-FPEL with F8BT/PS-*b*-PPP/SWNTs nanocomposite on a 100 nm thick PVP layer emitted light at both polarities when powered by a square-pulsed voltage of ±20 V at 30 kHz, as shown in Figure 5c. The results indicate that one type of carrier, which was injected from the top electrode to the SWNTs and was subsequently transferred to F8BT at a previous polarity, forms excitons with the other type of carrier injected from the SWNTs at a subsequent polarity, resulting in light emission. This process occurred successively for each of the two consecutive polarities, leading to luminescence at every polarity, as shown in Figure 5c. The luminescence at a certain polarity increased and reached a maximum at approximately 3 μs after the induction of a polarity; this is the characteristic time required for one type of carrier in F8BT to drift and recombine with the other type of carrier. Differences in the emission intensities at each polarity can be attributed to the different mobilities of the holes and electrons in F8BT, as reported previously.[32]

Because bipolar charges are injected dominantly through metallic SWNTs with a low contact energy barrier with the top electrode and then transferred to the nanocomposite in our SWNT-FPEL devices, there is great freedom in choice of the materials that can be used to design these types of devices, including the type of fluorescent emission polymer, insulator, and even top electrode. For instance, a SWNT-FPEL with an Al top electrode also exhibited EL performance comparable to that achieved with an Au electrode (see Supporting Information, Figure S4). Furthermore, the set of top and bottom electrodes and the insulating layer chosen for one type of fluorescent polymer can be also utilized for other polymers with different colors, as shown in the schematic of Figure 6. We successfully demonstrated red, green, and blue light emissions using poly[2-methoxy-5-(2-ethylhexyloxy)-1,4-phenylenevinylene] (MEH-PPV) (R), F8BT (G), and poly(9,9-di-n-octylfluorenyl-2,7-diyl) (PFO) (B), respectively, based on the unified device platform of ITO/PVP/(SWNTs/PS-*b*-PPP/fluorescent polymer)/Au, as shown in Figure 6. Our technique is therefore technologically advantageous, especially when considering that conventional OLEDs require elaborate energy band gap designs for each fluorescent polymer as well as several additional layers to aid in the charge injection and transfer of each electrode. Furthermore, flexible AC EL devices that incorporate an ITO bottom electrode sputtered onto a flexible substrate may contribute to the development of flexible, stretchable, electronics. Successive deposition of PVP insulator and our nanocomposite via spin-coating could be used to generate a flexible AC EL device after thermal evaporation of the Au top electrode.

To conclude, we manufactured and characterized a novel and high performance SWNT-FPEL device containing a SWNT/fluorescent polymer nanocomposite that emitted light under AC electric field excitation. The SWNT-FPEL device emitted light of approximately 350 cd/m^2 at an AC voltage of ±25 V and a frequency of 300 kHz because of SWNT-facilitated field-induced bipolar carrier generation. Holes and electrons were successively injected at each alternating electric field from the top electrode to the networked SWNTs in the composite and then transferred to light-emitting polymer layers. Subsequent exciton formation by the bipolar carriers resulted in greatly improved light emission upon recombination. Dispersal of individual SWNTs throughout the fluorescent polymer matrix, facilitated by the PS-*b*-PPP copolymer dispersant, was critical to achieve high performance EL. Our device emitted much brighter light than did other AC-based OELs and even inorganic ELs that operate at a few hundred volts. Furthermore, because our SWNT-FPEL device is based on field-induced bipolar charge injection, the material design rules are much simpler because there is no need to ensure energy band gap alignment between layers or to control carrier injection and transport, resulting in a very cost-effective device capable of full color emission.

■ ASSOCIATED CONTENT

Supporting Information. Additional information and figures. This material is available free of charge via the Internet at http://pubs.acs.org.

■ AUTHOR INFORMATION

Corresponding Author
*Tel: +82-2-2123-2833. Fax: +82-2-312-5375. E-mail: cmpark@yonsei.ac.kr.

■ ACKNOWLEDGMENT

This research was supported by the Converging Research Center Program through the Ministry of Education, Science, and Technology (No. 2010K001430). This project was also supported by The National Research Program for Memory Development, sponsored by the Ministry of Knowledge and Economy, Republic of Korea. In addition, this research was partly supported by the IT R&D program of MKE/KEIT (10030559, Development of next-generation high performance organic/nano materials and printing process technology) and by the Seoul R&BD Program (10816). Additional funding was provided by the Second Stage of the Brain Korea 21 Project in 2006 and through a National Research Foundation of Korea (NRF) grant, funded by the Ministry of Science and Technology (MEST), Republic of Korea (No. R11-2007-050-03001-0).

■ REFERENCES

(1) Müllen, K.; Scherf, U. *Organic Light-Emitting Devices: Synthesis, Properties and Applications*; Wiley-VCH: Weinheim, Germany, 2006.
(2) Reineke, S.; Lindner, F.; Schwartz, G.; Seidler, N.; Walzer, K.; Lussem, B.; Leo, K. *Nature* **2009**, *459*, 234.
(3) Hadziioannou, G.; Malliaras, G. G. *Semiconducting Polymers: Chemistry, Physics and Engineering*; Wiley-VCH: Weinheim, Germany, 2007.
(4) Friend, R. H.; Gymer, R. W.; Holmes, A. B.; Burroughes, J. H.; Marks, R. N.; Taliani, C.; Bradley, D. D. C.; Dos Santos, D. A.; Brédas, J. L.; Lögdlund, M.; Salaneck, W. R. *Nature* **1999**, *397*, 121.
(5) Ho, P. K.; Kim, J. S.; Burroughes, J. H.; Becker, H.; Li, S. F. Y.; Brown, T. M.; Cacialli, F.; Friend, R. H. *Nature* **2000**, *404*, 481.
(6) Kim, J. S.; Friend, R. H.; Grizzi, I.; Burroughes, J. H. *Appl. Phys. Lett.* **2005**, *87*, No. 023506.
(7) Zaumseil, J.; Friend, R. H.; Sirringhaus, H. *Nat. Mater.* **2006**, *5*, 69.
(8) Hepp, A.; Heil, H.; Weise, W.; Ahles, M.; Schmechel, R.; von Seggern, H. *Phys. Rev. Lett.* **2003**, *91*, No. 157406.
(9) Muccini, M. *Nat. Mater.* **2006**, *5*, 605.
(10) Destriau, G. *J. Chim. Phys.* **1936**, *33*, 587.
(11) Krupka, D. C. *J. Appl. Phys.* **1972**, *43*, 476.
(12) Zheng, X.; Feng, T.; Chong, Q.; Suling, Z.; Xurong, X. *Physica B* **2004**, *348*, 231.
(13) Yang, S. Y.; Qian, L.; Teng, F.; Xu, Z.; Xu, X. R. *J. Appl. Phys.* **2005**, *97*, No. 126101.
(14) Xu, X. L.; Chen, X. H.; Hou, Y. B.; Xu, Z.; Yang, X. H.; Yin, S. G.; Wang, Z. J.; Xu, X. R.; Lau, S. P.; Tay, B. K. *Chem. Phys. Lett.* **2000**, *325*, 420.
(15) Gu, G.; Parthasarathy, G.; Burrows, P. E.; Tian, P.; Hill, I. G.; Kahn, A.; Forrest, S. R. *J. Appl. Phys.* **1999**, *86*, 4067.
(16) Tsutsui, T.; Lee, S.; Fujita, K. *Appl. Phys. Lett.* **2004**, *85*, 2382.
(17) Avouris, P.; Martel, R. *MRS Bull.* **2010**, *35*, 306.
(18) Chen, J.; Perebeinos, V.; Fretag, M.; Tsang, J.; Fu, Q.; Liu, J.; Avouris, P. *Science* **2005**, *310*, 1171.
(19) Marty, L.; Adam, E.; Albert, L.; Doyon, R.; Menard, D.; Martel, R. *Phys. Rev. Lett.* **2006**, *96*, No. 136803.
(20) Xu, Z.; Wu, Y.; Hu, B.; Ivanov, I. N.; Geohegan, D. B. *Appl. Phys. Lett.* **2005**, *87*, No. 263118.
(21) Fournet, P.; O'Brien, D. F.; Coleman, J. N.; Hörhold, H.-H.; Blau, W. J. *Synth. Met.* **2001**, *121*, 1683.
(22) Woo, H. S.; Czerw, R.; Webster, S.; Carroll, D. L.; Ballato, J.; Strevens, A. E.; O'Brien, D.; Blau, W. J. *Appl. Phys. Lett.* **2000**, *77*, 1396.
(23) Lee, K. W.; Lee, S. P.; Choi, H.; Mo, K. H.; Jang, J. W.; Kweon, H.; Lee, C. E. *Appl. Phys. Lett.* **2007**, *91*, No. 023110.
(24) Bae, M. J.; Park, S. H.; Jeong, T. W.; Lee, J. H.; Han, I. T.; Jin, Y. W.; Kim, J. M.; Kim, J. Y.; Yoo, J. B.; Yu, S. G. *Appl. Phys. Lett.* **2009**, *95*, No. 071901.
(25) Sung, J.; Huh, J.; Choi, J.-H.; Kang, S. J.; Choi, Y. S.; Lee, G. T.; Cho, J.; Myoung, J.-M.; Park, C. *Adv. Func. Mater.* **2010**, *20*, 4305.
(26) Moniruzzaman, M.; Winey, K. I. *Macromolecules* **2006**, *39*, 5194.
(27) Schuettfort, T.; Snaith, H. J.; Nish, A.; Nicholas, R. J. *Nanotechnology* **2010**, *21*, No. 025201.
(28) Avouris, P.; Chen, Z.; Perebeinos, V. *Nat. Nanotechnol.* **2007**, *2*, 605.
(29) Du1rkop, T.; Getty, S. A.; Cobas, E.; Fuhrer, M. S. *Nano Lett.* **2004**, *4*, 35.
(30) Bringuier, E. *J. Appl. Phys.* **1991**, *70*, 4505.
(31) Lee, T.-W.; Zaumseil, J.; Kim, S. H.; Hsu, J. W. P. *Adv. Mater.* **2004**, *16*, 2040.
(32) Brückner, J.; Christ, N.; Bauder, O.; Gärtner, C.; Seyfried, M.; Glöckler, F.; Lemmer, U.; Gerken, M. *Appl. Phys. Lett.* **2010**, *96*, No. 041107.